Zn^+ Implanted Silicon Waveguide Photodiodes for On-Chip Mid-Infrared Detection

Richard R. Grote,[1,*] Brian Souhan,[1] Noam Ophir,[2] Jeffrey B. Driscoll,[1] Keren Bergman,[2] Hassaram Bakhru,[3] William M. J. Green,[4] and Richard M. Osgood, Jr.[1]

[1]*Microelectronics Sciences Laboratories, Columbia University, New York, NY 10027, USA*
[2]*Department of Electrical Engineering, Columbia University, 500 W. 120th Street, New York, NY 10027, USA*
[3]*College of Nanoscale Science and Engineering, State University of New York at Albany, Albany, NY 12203, USA*
[4]*IBM T. J. Watson Research Center, 1101 Kitchawan Rd., Yorktown Heights, NY 10598, USA*
[*]*rrg2130@columbia.edu*

Abstract: We present the first experimental demonstration of Zn^+ implanted Si waveguide photodiodes for 2.2-2.4 μm operation. Preliminary responsivities > 65 mA/W are measured, suggesting suitability for on-chip sensing and communications applications in the mid-infrared.

OCIS codes: (040.6040) Silicon; (040.5160) Photodetectors; (040.3060) Infrared; (130.3060) Infrared.

1. Introduction

Silicon photonics has recently been proposed for a diverse set of applications in the mid-infrared (λ = 2-5 μm), including spectroscopy, chemical and biological sensing, free-space communications, and non-linear optics [1,2]. On-chip mid-infrared waveguide-integrated detectors are extremely beneficial for photonic integrated circuits targeted at these applications. A number of such detectors have been demonstrated, including heterogeneously integrated GaSb [3], PbTe colloidal quantum dots [3], and PbTe photoconductors with chalcogenide glass waveguides [4]. An alternate method for photodetection beyond the band edge of Si is to introduce optically absorbing defect states within the bandgap via ion-implantation. This method, which alleviates the need for heterogeneous integration, has recently been demonstrated with high-performance photodiodes (PDs) at 1.55 μm [5-7] and 1.9 μm [8]. For the 2.2-2.4 μm wavelength range, Zn^+ implantation has been shown to produce a suitable defect level in Si and has been studied in the form of bulk photoconductive detectors [9].

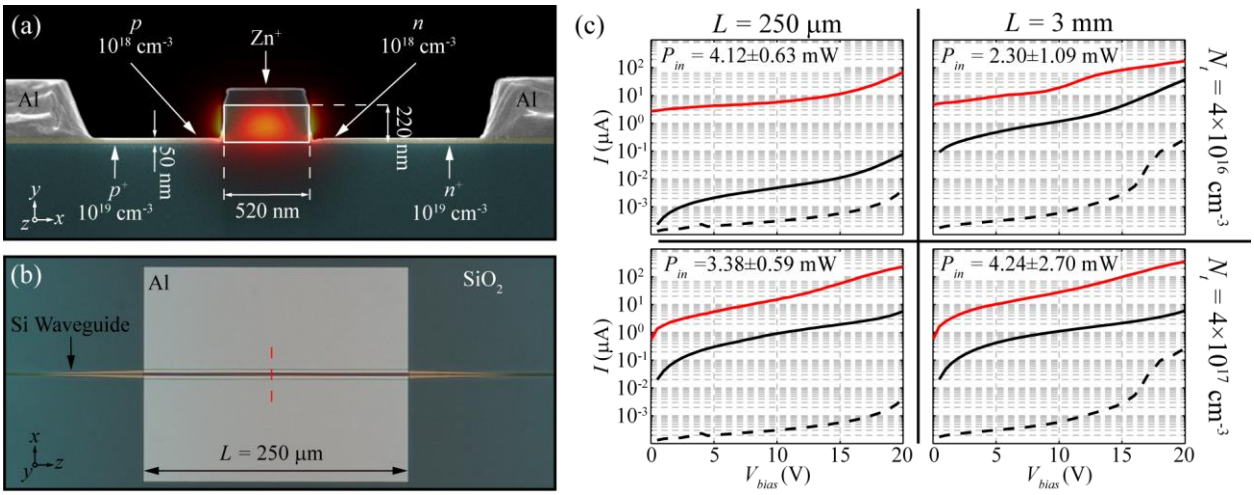

Fig. 1. (a) False color SEM cross-section of the Si waveguide PD with finite-element-method calculated mode intensity at λ = 2.3 μm superimposed. The waveguide has a 90 nm SiO_2 hardmask and 3 μm buried-oxide-layer substrate. (b) Top-view optical microscope image of the PD, red dashed line indicates the position of the SEM cross-section shown above. (c) Photocurrent (——), dark current (——), and dark current from an un-implanted reference device (– –) for two different PD lengths and defect concentrations at λ = 2.2 μm.

Here, we present the first experimental demonstration of Zn^+ implanted Si waveguide PDs for mid-infrared detection. The PDs are based on a *p-i-n* diode structure (cross-sectional SEM shown in Fig. 1a, top-view shown in Fig. 1b). Two Zn^+ implantation dosages and PD lengths are measured: 10^{12} cm^{-2} and 10^{13} cm^{-2}, corresponding to estimated average defect concentrations of $N_t = 4\times10^{16}$ cm^{-3} and $N_t = 4\times10^{17}$ cm^{-3}, respectively, and L = 250 μm, 3 mm. The photocurrent as a function of reverse bias voltage from each of these devices is shown in Fig. 1c. Our results represent a crucial step towards the development of high-performance Si-based PDs for the mid-infrared, with detection being extendable to longer wavelengths by appropriate choice of the implantation species.

2. Results and Discussion

The un-implanted devices were fabricated as described in [5], and were subsequently masked to define implant windows using contact photolithography. The structures were then implanted with Zn^+ at an acceleration voltage of 260 KeV. Post-implantation, the devices were annealed at 350°C for 10 minutes on a hot plate in ambient conditions. The photocurrent versus bias voltage was measured with an external-cavity Cr^{2+}:ZnSe tunable laser at a series of wavelengths from 2.2-2.4 μm in 25 nm steps, and the transmitted power T was monitored on an optical spectrum analyzer. The measurements were repeated for an un-implanted diode (having identical p and n implants and contact metallization as the Zn^+ implanted PD), allowing for the effects of parasitic absorption in the Al contacts to be taken into account.

The responsivity, defined as $R = (I_{ph}\text{-}I_{dark})/P_{in}$ [A/W], where I_{ph} is the photocurrent generated under illumination, I_{dark} is the dark current, and P_{in} is the on-chip power entering the detector, is shown in Fig. 2a for a series of increasing bias voltages. The error bars have been determined based on fluctuations in the transmitted power and variations in fiber-to-chip coupling losses. R is largest at shorter wavelengths in all cases, and increases with device length. The modal absorption coefficient, $\alpha_{eff} = -T/L$ [dB/cm], is determined with L = 250 μm. By subtracting the parasitic absorption coefficient $\alpha_{eff,par}$, measured from an un-implanted diode, from the absorption coefficient of a Zn^+ implanted PD, $\alpha_{eff,tot}$, the absorption coefficient due to defects (Fig. 2b) is determined: $\alpha_{eff,Zn} = \alpha_{eff,tot} - \alpha_{eff,par}$. The fraction of total loss due to parasitic absorption and defect absorption are plotted versus wavelength in Fig. 2c, from which it is clear that the contact absorption becomes dominant for $\lambda > 2.325$ μm. By moving the contacts further from the waveguide, R can be greatly improved at longer wavelengths. Similarly, other methods for increasing R of the PDs such as compensation doping and higher post-implantation annealing temperatures are currently being explored.

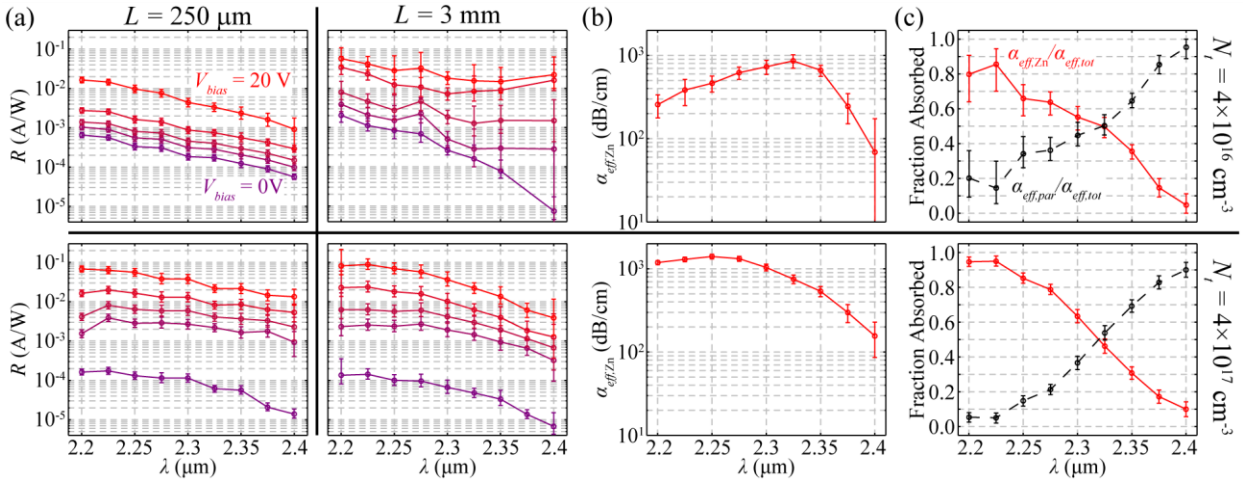

Fig. 2. (a) Measured responsivity versus wavelength with increasing bias voltage from 0V (—∘—) to 20V (—∘—) in 5V increments. (b) Measured absorption coefficient due to implantation versus wavelength. (c) Measured fractional absorption due to implantation (—∘—), and parasitic contact loss (–∘–). Contact loss becomes dominant at longer wavelengths, resulting in decreased responsivity. For (a)-(c) top panels correspond to $N_t = 4\times10^{16}$ cm^{-3} and bottom panels correspond to $N_t = 4\times10^{17}$ cm^{-3}.

3. Conclusion

We have demonstrated integrated mid-infrared detectors using Zn^+ implanted Si waveguide PDs with low dark currents and responsivities of > 65 mA/W. By increasing the post-implantation annealing temperature, R can be increased further. Detection can be extended to longer wavelengths by choosing an appropriate implantation species and by designing the contacts such that the parasitic losses are minimized. These PDs represent the first step towards a high-performance component for mid-infrared Si photonic applications.

This research was carried out in part at the Center for Functional Nanomaterials, Brookhaven National Laboratory, which is supported by the U.S. Department of Energy, Office of Basic Energy Sciences, under Contract No. DE-AC02-98CH10886. The authors acknowledge support from the Columbia Optics and Quantum Electronics IGERT under NSF Grant DGE-1069420, and thank M. W. Geis and S. Spector for diode design and fabrication.

[1] R. Soref, "Mid-infrared photonics in silicon and germanium," Nature Photonics **4**, 495-497 (2010).
[2] X. Liu, R. M. Osgood, Jr., Y. A. Vlasov, and W. M. J. Green, "Mid-infrared optical parametric amplifier using silicon nanophotonic waveguides," Nature Photonics **4**, 557-560 (2010).
[3] G. Roelkens *et al.*, "Silicon-based heterogeneous photonic integrated circuits for the mid-infrared," Opt. Mater. Express **3**, 1523-1536 (2013).
[4] P. T. Lin *et al.*, "Si-CMOS compatible materials and devices for mid-IR microphotonics," Opt. Mater. Express **3**, 1474-1487 (2013).
[5] M. W. Geis *et al.*, "All silicon infrared photodiodes: photo response and effects of processing temperature," Opt. Express **15**, 16886-16895 (2007).
[6] R. R. Grote *et al.*, "10 Gb/s Error-Free Operation of All-Silicon Ion-Implanted-Waveguide Photodiodes at 1.55 μm," IEEE Photon. Technol. Lett. **25**, 67-70 (2013).
[7] J. J. Ackert *et al.*, "10 Gbps silicon waveguide-integrated infrared avalanche photodiode," Opt. Express **21**, 19530-19537 (2013).
[8] B. Souhan *et al.*, "Error-Free Operation of an All-Silicon Waveguide Photodiode at 1.9 μm," IEEE Photon. Technol. Lett. **25**, 2031-2034 (2013).
[9] N. Sclar, "Properties of High Performance Background Limited *p* Type Si:Zn Photoconductors," Solid-State Electronics **24**, 203-213 (1981).